Commun Nonlinear Sci Numer Simulat 30 (2016) 101–107

Contents lists available at ScienceDirect

Commun Nonlinear Sci Numer Simulat

journal homepage: www.elsevier.com/locate/cnsns

Sensitivity to initial conditions of the self-trapping transition in C_{60} buckyballs with relaxing nonlinearity

A.F.G. Silva [a], R.P.A. Lima [a,b], V.L. Chaves Filho [a,c], F.A.B.F. de Moura [a], M.L. Lyra [a,*]

[a] GFTC, Instituto de Física, Universidade Federal de Alagoas, Maceió AL 57072-970, Brazil
[b] GISC, Instituto de Física, Universidade Federal de Alagoas, Maceió AL 57072-970, Brazil
[c] Instituto Federal de Educação, Ciência e Tecnologia de Alagoas, Satuba AL 57120-000, Brazil

ARTICLE INFO

Article history:
Received 23 December 2014
Revised 9 April 2015
Accepted 1 June 2015
Available online 9 June 2015

Keywords:
C_{60} buckyballs
Third-order nonlinearity
Wavepacket dynamics
Self-trapping transition

ABSTRACT

We study the one-electron wavepacket dynamics in a C_{60} buckyball topology with a relaxing nonlinearity. The electron dynamics is considered to be governed by a discrete Schrödinger equation on which the nonlinear contribution obeys a Debye-like relaxation process. We follow the temporal evolution of the wavepacket and use the associated participation number to probe its spatial extension. By considering distinct initial conditions, we characterize the delocalization/self-trapping transition as a function of the nonlinear strength and relaxation time. We show that the phase-diagram exhibits a complex pattern of tongues signaling a re-entrant behavior of the transition which is strongly sensitive to the initial wavepacket distribution. The re-entrances become less prominent for initial conditions which are spatially distributed over opposite clusters.

1. Introduction

Wave propagation in low-dimensional nonlinear models is a timely subject with several connections with basic and applied solid state physics, optics, acoustics, and Bose–Einstein condensation, among others [1–22,24–29]. Within the context of electronic transport in low-dimensional nonlinear discrete lattices, one of the most known properties is the self-trapping (ST) phenomena. In general lines, ST occurs when the strength of the nonlinearity surpasses a threshold which is of the order the bandwidth for initially fully localized wavepackets [2–6]. In this case, the electron wavepacket remains trapped around the initial position with the probability of finding the electron at its initial position remaining finite in the long-time limit. Some specificities of the ST transition in square and honeycomb lattices were reported in [7] showing that the ST threshold continuously grows as a function of the initial wavepacket width. Recent experiments have probed the electron–phonon interaction in graphene [30,31] and mapped the wavefunction in graphene quantum dots [32–34]. Low-temperature scanning tunneling microscopy experiments can thus be explored to directly observe theoretical predictions concerning the wavepacket dynamics in carbon-based structures.

A question that has attracted recent interest concerns the role played by the finite nonlinear response time on the wavepacket dynamics in discrete lattices. In Ref. [6] the problem of electronic ST in a chain with a non-adiabatic delayed electron–phonon coupling was investigated. It was shown that, in the regime of short delay times, a weaker nonlinearity is required to promote the ST transition when compared with the case of an instantaneous response. It was also demonstrated that for slowly responding

* Corresponding author. Tel.: +55 82 32144232/+55 82 3214 1432; fax: +55 82 3214 1645.
E-mail address: marcelo@fis.ufal.br, marcelo@if.ufal.br (M.L. Lyra).

http://dx.doi.org/10.1016/j.cnsns.2015.06.002
1007-5704/

media, ST only takes place for very strong nonlinearities. By using a Debye-like law for the relaxation of the nonlinearity, it was shown that the slow relaxation of the nonlinearity is responsible for the reduction of the delocalized regime and for the emergence of a complex wavepacket self-focusing regime [22]. The competition between disorder and a finite nonlinear response time was investigated in Ref. [23]. It was numerically demonstrated that no sub-diffusive spreading of the second moment of the wavepacket distribution takes place when the finite response time of the nonlinearity is taken into account. Such re-localization was latter explained as resulting from the energy drift towards the band edge [24]. More recently, it has been evidenced that the relaxation process of the nonlinearity has a profound impact in the wavepacket dynamics and in the formation of self-trapped stationary states in C_{60} buckyballs [27]. In this structure, finite-size effects play a major role in the wavepacket dynamics.

In the present work, we will unveil the influence of the initial wavepacket distribution on the self-trapping transition in the C_{60} topology in the presence of a non-instantaneous nonlinearity. By considering a discrete nonlinear Schrödinger equation within a non-adiabatic approximation, we will analyze the dynamics of a one-electron wavepacket having distinct initial distributions. We will present the phase diagram as a function of the nonlinear coupling and the relaxation time of the nonlinearity. In particular, we will show that the wavepacket dynamics depicts re-entrant behaviors both as a function of the strength of the nonlinear coupling and as a function of the relaxation time. This leads to a complex structure of tongues in the phase-diagram that becomes less prominent when wider initial wavepackets distributed in disconnected clusters are considered.

2. Model and formalism

In the following, we will analyze the one-electron wavepacket dynamics on a C_{60} buckyball topology. We will consider that the intrinsic vibrations of the lattice do not reach equilibrium as compared with the time-evolution of the electron wavepacket. Under this condition, a non-adiabatic framework has to be employed to account for the relaxation of the effective nonlinear term resulting from the underlying electron–lattice coupling.

The discrete nonlinear Schrödinger equation appears within the electron–lattice interaction picture in an Einstein-like model of the lattice vibrations [35] whose Hamiltonian can be written as

$$H = \sum_n \left[\frac{p_n^2}{2M} + \frac{M\omega_0^2 u_n^2}{2} \right] + \sum_{(n,m)} V_{n,m} a_n^\dagger a_m + U \sum_n u_n a_n^\dagger a_n, \tag{1}$$

where the first term is associated with local harmonic oscillators with mass M and Einstein frequency ω_0 (u_n and p_n stand for the vibrational displacement and its conjugated momentum, respectively). The on-site electron energy is set to zero without loss of generality. The second sum corresponds to the electron hopping integral between first neighbor sites (n, m). The C_{60} buckyball has 60 sites distributed in 20 hexagons and 12 pentagons. Each site has three bonds, two of them between a hexagon and a pentagon (single bonds) and the other between two hexagons (π bonds). Although these two types of bonds have slightly different lengths, we will consider that the hopping amplitude V_{nm} is the same irrespective to the bond type. It will be taken as unitary hereafter. The third term accounts for the electron–lattice coupling of strength U. $a_n^\dagger$ and a_n are creation and annihilation fermion operators. In the absence of electron–phonon coupling, the one-electron eigen-energies and the structure of the eigenstates were investigated in the previous literature [36]. An exact diagonalization of the Hamiltonian matrix shows that, although most of the eigenstates are not uniformly distributed over the buckyball, they are spread over a significant fraction of the sites. By decomposing the electronic quantum state in the local Wannier basis set ($|\Psi\rangle = \sum_n \Psi_n |n\rangle$), the time-evolution of the electronic wavefunction amplitudes is given by

$$i\dot{\Psi}_n(t) = \sum_m V_{nm}\Psi_m(t) - X_n(t)\Psi_n(t), \tag{2}$$

in units of $\hbar = 1$. A variational treatment provides that the minimal eigen-energies are achieved for the stationary value $X_n = \frac{U^2}{M\omega_0^2}|\Psi_n|^2$ [37], thus resulting in an effective discrete nonlinear Schrödinger equation, with the nonlinear parameter $\chi = \frac{U^2}{M\omega_0^2}$ accounting for the underlying electron–lattice coupling. Here, we will consider the relaxation process of the nonlinearity assuming that the lattice oscillations are over-damped. In this way, its relaxation towards the stationary value is governed by a single time scale τ characterizing a Debye-like process described by

$$\dot{X}_n(t) = -\frac{1}{\tau}[X_n(t) + \chi|\Psi_n(t)|^2]. \tag{3}$$

To probe the wavepacket dynamics, we will follow the time-evolution of the participation number $P(t)$ defined as

$$P(t) = \left[\sum_j |\Psi_j|^4 \right]^{-1}. \tag{4}$$

In general, the participation number is used as an estimate of the number of sites that effectively contribute to the electronic probability distribution. For uniformly extended states, $P(t)$ equals the total number of sites N. For strongly localized states, the participation number becomes much smaller than N.

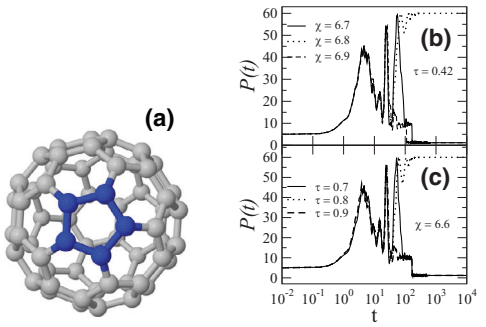

Fig. 1. (a) Illustration of the initial wavepacket uniformly distributed over the sites of a pentagon. (b–c) Some representative time-dependent participation function for (b) $\tau = 0.42$ and $\chi = 6.7, 6.8, 6.9$; (c) $\chi = 6.6$ and $\tau = 0.7, 0.8, 0.9$. There appears an alternate sequence of localization and self-trapping as a function of both χ and τ.

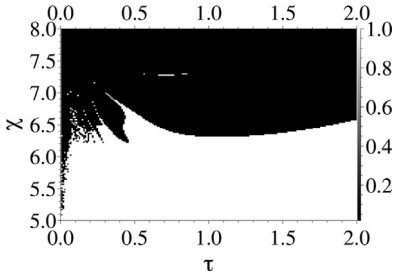

Fig. 2. The phase diagram within the two-dimensional parameter space τ, χ. Black region indicates the self-trapped regime and the white region accounts for fully delocalized states. The transition between these two regimes is discontinuous. Calculations were done for the case in which the wavepacket is initially uniformly distributed over the sites of a pentagon.

3. Results and discussions

We numerically solved the model equations by considering several distinct kinds of initial conditions using a standard eight-order Runge–Kutta algorithm [38] with time step $dt = 0.005$. We did not find any significant quantitative or qualitative difference for time discretizations $dt \ll 0.005$ or by solving the nonlinear equations using alternative numerical methods. The numerical convergence and stability were checked at each time step. We verified that the norm conservation, e.g. $(|1 - \sum_n |\Psi_n|^2| < 10^{-7})$ was satisfied during the entire simulation time.

We followed the time evolution of the wavepacket until it has reached a stationary regime. We start by showing our results for the case in which the wavepacket is initially distributed uniformly over the sites of a pentagon, as illustrated in Fig. 1a. The temporal evolution of the participation function is reported for some typical sets of model parameters (namely the strength of the nonlinearity χ and the relaxation time τ) (see Fig. 1b–c). In all cases, the initial wavepacket has a participation number $P(t = 0) = 5$, according to the initial wavepacket distribution over the pentagon. In Fig. 1b, we fixed the relaxation time and varied the nonlinear strength over values close to the transition from delocalized to self-trapped states. Notice that the oscillations taking place at intermediate times, which signal the emergence of irregular breathings, are weakly sensitive to the precise value of the nonlinear strength. However, the convergence to the ultimate stationary state strongly depends on χ. For small nonlinearities, the stationary state is uniformly distributed over all sites of the buckyball, while it focuses over very few sites for strong nonlinearities. It is worth to call attention to the fact that the transition from delocalized to self-trapped states that takes place with increasing strengths of the nonlinearity depicts a re-entrant behavior, characterized by an alternate sequence of self-trapped and delocalized asymptotic wavepackets. In Fig. 1c we explore the dependence of the wavepacket time-evolution on the relaxation time τ. Here we fixed the nonlinear coupling at a value close to the delocalization/self-trapped transition and report results for some representative values of the relaxation time. We also observe that the initial transient oscillations are weakly sensitive to the actual precise value of τ, in contrast to the participation number of the asymptotic wavepacket. The re-entrant behavior of the transition as a function of τ is also evidenced. In Fig. 2 we provide the full phase diagram in the parameter space $\chi \times \tau$. The region in white corresponds to asymptotic participation $P/N = 1$ (fully extended wavepacket) while the region in black to P/N near zero (well localized wavepacket). Intermediate values would appear in gray scale between these two limiting values. The absence of asymptotic intermediate values of the participation number signals that the transition from localized to extended asymptotic states is discontinuous. The re-entrant behavior of the transition is reflected by the emergence of several tongues, which become quite fragmented in the regime of short relaxation times. In this regime, there is a strong sensitivity of the asymptotic state on the precise values of the model parameters.

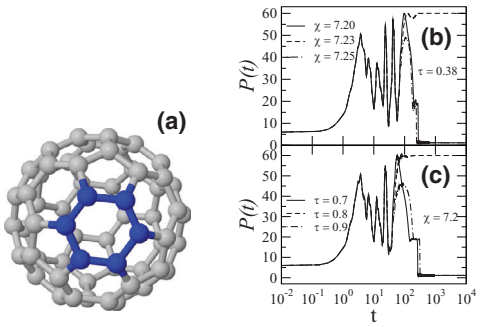

Fig. 3. (a) Illustration of the initial wavepacket distributed uniformly over the sites of an hexagon. (b–c) Some representative time-dependent participation function for (b) $\tau = 0.38$ and $\chi = 7.20, 7.23, 7.25$; (c) $\chi = 7.2$ and $\tau = 0.7, 0.8, 0.9$. Notice the alternate sequence of localization and self-trapping as a function of both χ and τ.

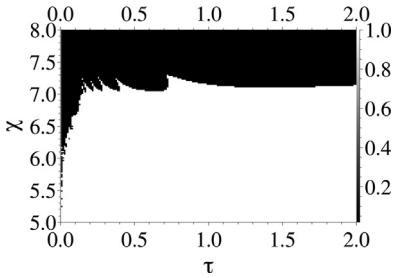

Fig. 4. The phase diagram regarding the self-trapped (black region) and the delocalized (white region) regimes in the two-dimensional parameter space (τ, χ). Calculations were done for the case in which the wavepacket is initially uniformly distributed over the sites of an hexagon.

In order to explore the sensitivity on the initial condition of the delocalization/self-trapping transition, we now consider the case on which the wavepacket is initially distributed uniformly over the sites of an hexagon, as illustrated in Fig. 3a. We also show some representative time evolution series of the participation number (see Fig. 3b–c). The transition also depicts a re-entrant behavior, either as a function of the nonlinear strength (Fig. 3b) or as a function of the relaxation time (Fig. 3c). The corresponding phase diagram is shown in Fig. 4. Although it has a similar structure as the one attained for the pentagonal initial condition, there are a few characteristics that deserve to be stressed. Firstly, the re-entrances are less pronounced for the hexagonal initial condition. However, the sequence of tongues is more clearly defined, pointing for a weaker sensitivity on the model parameters in the regime of short relaxation times. Further, the critical nonlinear strength in the regime of slowly responding nonlinearity ((large τ) is somewhat larger than the one obtained for the pentagonal initial condition. This feature is in agreement with previous results concerning the self-trapping transition which showed a monotonic increase of the self-trapping threshold when the width of the initial wavepacket distribution is increased [7].

Before concluding, we consider other kinds of initial conditions (see Fig. 5): (a) extended pentagon, (b) two opposite pentagons, (c) extended hexagon, and (d) two opposite hexagons. The extended pentagon initial condition consists of the wavepacket initially distributed uniformly over 10 sites: those of a pentagon and its five nearest neighboring sites, as illustrated in Fig. 5a. The two opposite pentagons initial condition also consists of the wavepacket distributed uniformly over 10 sites, but distributed in opposite clusters (see Fig. 5b). In the extended hexagon initial condition, the wavepacket is initially distributed over 12 sites occupying an hexagon and its nearest neighbors, as shown in Fig. 5c, while in the two opposite hexagons initial condition the 12 sites occupy diametrically opposite hexagonal clusters (see Fig. 5d). Representative plots of the participation number time-evolution for each one of these initial conditions are shown in Fig. 6. In all cases, the participation depicts a direct transition between well localized and fully extended asymptotic states. The location of the asymptotically localized state is strongly dependent on the initial condition and model parameters, especially near the localization–delocalization transition.

In Fig. 7, we report the phase diagrams resulting from each one of the above initial conditions. For the extended pentagon (Fig. 6a) and hexagon (Fig. 6c) initial conditions, the phase diagrams are quite similar to those obtained for wavepackets distributed initially over the corresponding closed clusters. The main difference is that the re-entrant tongues are slightly less pronounced. On the other hand, the phase diagrams related to the initial conditions with the wavepacket distributed in opposite clusters are quite distinct, even though they have the same initial participation number as their extended cluster counterpart. In these cases (see Fig. 6b and d) the re-entrant tongues are absent. The threshold nonlinear coupling separating delocalized from self-trapped asymptotic wavepackets are roughly independent of the relaxation time, except in the regime of very fast nonlinear responses on which the self-trapping threshold displays a small decrease (visible in Fig. 6b). This feature is due to the fact that, for these initial conditions the wavepacket spreads over the entire buckyball in a shorter time than in the case of an initially connected single cluster. In this case, the transition from delocalization to self-trapping is triggered by the modulational instability

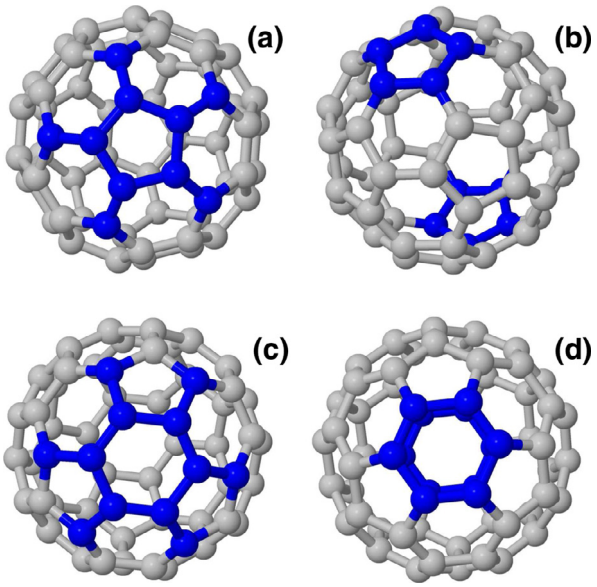

Fig. 5. Illustrative representations of 4 distinct initial conditions with the wavepacket distributed uniformly over the sites of (a) an extended pentagon, (b) two opposite pentagons, (c) an extended hexagon, and (d) two opposite hexagons. .

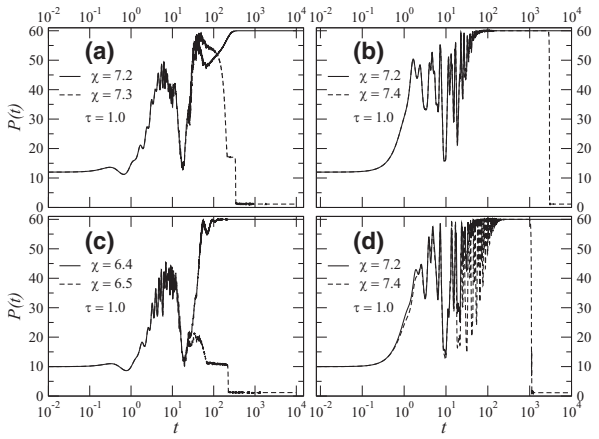

Fig. 6. Some representative time-dependent participation functions for distinct initial conditions: (a) Extended pentagon; (b) Extended hexagon; (c) Opposite pentagons; and (d) Opposite hexagons. In all cases, the transition from well localized to fully extended asymptotic states is direct.

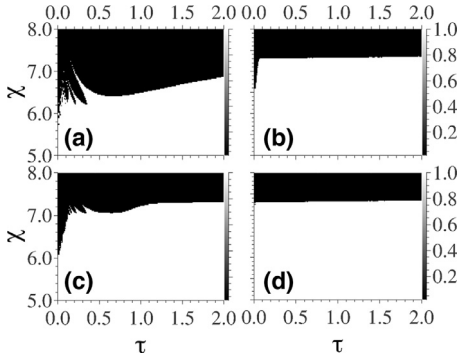

Fig. 7. The phase diagrams within the two-dimensional parameter space τ, χ. Calculations were done by considering four distinct types of initial conditions: (a) extended pentagon (b) two opposite pentagons (c) extended hexagon and (d) two opposite hexagons. Notice that the re-entrances are absent when the initial wavepacket is distributed in opposite clusters. .

of the uniform solution. The asymptotic threshold is also larger than in the cases of single connected clusters, corroborating its expected dependence on the initial participation number [7].

4. Summary and conclusions

In summary, we investigated the time-evolution of one-electron wavepackets restricted to evolve on the sites of a C_{60} buckyball under the influence of a third-order nonlinearity with a finite relaxation time τ. Within a tight-binding approach including a Debye-like relaxation process of the nonlinear contribution, we provided a detailed study of the transition from delocalized to self-trapped asymptotically stationary states. In the regime of weak nonlinear couplings, the asymptotic state becomes delocalized irrespective to the nonlinear relaxation time and initial condition. On the other hand, the wavepacket evolves to a self-trapped stationary state for strong nonlinearities. However, we unveiled that the actual location of the transition is strongly dependent on the initial condition as well on the relaxation time of the nonlinearity.

We provided the full phase-diagram for six distinct initial conditions. In four of them, we considered that the wavepacket was initially uniformly distributed over the sites of a connected cluster (pentagon, hexagon, extended pentagon, and extended hexagon). In all of these cases, the phase diagram presents re-entrant tongues reflecting the presence of a sequence of transitions when increasing the nonlinear strength, before the ultimate self-trapping. These re-entrances are more prominent in the short relaxation time regime, as well as in the smallest initial cluster. Such re-entrant phase-diagram indicates that the border between the dynamical attractors related to localized and extended states is complex, as usual in high-dimensional nonlinear dynamical systems (120 dynamical variables in the present model). Further, in the range of nonlinear strengths corresponding to this re-entrant behavior, a sequence of self-trapping to delocalization transitions can also take place with increasing relaxation times. For the initial conditions on which the wavepacket is distributed in disconnected opposite clusters (opposite pentagons and hexagons) the re-entrant behavior of the transition is suppressed and the nonlinear threshold signaling the self-trapping transition becomes roughly independent of the nonlinear relaxation time. In this case, the self-trapping transition occurs after the initial spread of the wavepacket over the entire buckyball and is triggered by the modulational instability of the uniform solution.

The above phenomenology shall also appear in general nonlinear physical systems where the wavepacket dynamics is influenced by a relaxing nonlinearity. Extensions of the present study to other nanosized clusters with strong electron–phonon coupling, BEC in optical lattices, as well as of light propagation in nonlinear photonic crystals would be in order to provide a more complete scenario regarding the physical mechanisms behind the self-trapping transition in slowly responding nonlinear lattices.

Acknowledgments

This work was partially supported by CNPq, CAPES (Grant no. PVE-A121), and FINEP (Federal Brazilian Agencies), as well as FAPEAL (Alagoas State Agency). The authors would like to thanks HPC-Lattes (UNILA) for providing computational facilities.

References

[1] Hennig D, Tsironis GP. Phys Rep 1999;307:333.
[2] Kopidakis G, Soukoulis CM, Economou EN. Europhys Lett 1996;33:459.
[3] Kopidakis G, Soukoulis CM, Economou EN. Phys Rev B 1995;51:15038.
[4] Ivanchenko MV. Phys Rev Lett 2009;102:175507; Flach S, Krimer DO, Skokos Ch. Phys Rev Lett 2009;102:024101; Skokos Ch, Krimer DO, Komineas S, Flach S. Phys Rev E 2009;79:056211; Sangiovanni G, Capone M, Castellani C, Grilli M. Phys Rev Lett 2005;94:026401.
[5] Dias WS, Lyra ML, de Moura FABF. Eur Phys J B 2012;85:7.
[6] de Moura FABF, Gléria I, dos Santos IF, Lyra ML. Phys Rev Lett 2009;103:096401.
[7] Dias WS, Lyra ML, de Moura FABF. Phys Rev B 2010;82:233102.
[8] Kopidakis G, Komineas S, Flach S, Aubry S. Phys Rev Lett 2008;100:084103; Pikovsky AS, Shepelyansky DL. Phys Rev Lett 2008;100:094101; Hajnal D, Schilling R. Phys Rev Lett 2008;101:124101; Lahini Y, Avidan A, Pozzi F, Sorel M, Morandotti R, Christodoulides DN, Silberberg Y. Phys Rev Lett 2008;100:013906.
[9] de Moura FABF, Caetano RA, Santos B. J Phys: Condens Matter 2012;24:245401.
[10] Davydov AS. Solitons in molecular systems. 2nd ed. Dordrecht: Reidel; 1991.
[11] Scott AC. Phys Rep 1992;217:1.
[12] Davydov AS. Phys Scr 1979;20:387.
[13] Davydov AS. J Theor Biol 1977;66:379.
[14] Davydov AS. Biology and quantum mechanics. New York: Pergamon; 1982.
[15] Brizhik L, Chetverikov AP, Ebeling W, Ropke G, Velarde MG. Phys Rev B 2012;85:245105.
[16] Chetverikov AP, Ebeling W, Velarde MG. Physica D 2011;240:1954.
[17] Hennig D, Velarde MG, Ebeling W, Chetverikov AP. Phys Rev E 2008;78:066606.
[18] Makarov VA, Velarde MG, Chetverikov AP, Ebeling W. Phys Rev E 2006;73:066626.
[19] Hennig D, Neissner C, Velarde MG, Ebeling W. Phys Rev B 2006;73:024306.
[20] Ebeling W, Chetverikov AP, Röpke G, Velarde MG. Contrib Plasm Phys 2013;53:736.
[21] Sales MO, de Moura FABF. J Phys: Condens Matter 2014;26:415401.
[22] de Moura FABF, Vidal EJGG, Gleria I, Lyra ML. Phys Lett A 2010;374:4152.
[23] Caetano RA, de Moura FABF, Lyra ML. Eur Phys J B 2011;80:321.
[24] Mulansky M, Pikovsky AS. Eur Phys J B 2012;85:105.
[25] Kenkre VM, Wu H-L. Phys Rev B 1989;39:6907.
[26] Grigolini P, Wu H-L, Kenkre VM. Phys Rev B 1989;40:7045.
[27] Lyra ML, Lima RPA. Phys Rev E 2012;85:057201.

[28] Tian S-F, Zu L, Ding Q, Zhang H-Q. Commun Nonlinear Sci Numer Simulat 2012;17:3247.
[29] Tawfik SA. Commun Nonlinear Sci Numer Simulat 2012;17:3552.
[30] Bianchi M, Rienks EDL, Lizzit S, Baraldi A, Balog R, Hornekaer L, Hofmann Ph. Phys Rev B 2010;81:041403.
[31] Grüneis A, Attaccalite C, Rubio A, Vyalikh DV, Molodtsov SL, Fink J, Follath R, Eberhardt W, Büchner B, Pichler T. Phys Rev B 2009;79:205106.
[32] Subramaniam D, Libisch F, Li Y, Pauly C, Geringer V, Reiter R, Mashoff T, Liebmann M, Burgdörfer J, Busse C, Michely T, Mazzarello R, Pratzer M, Morgenstern M. Phys Rev Lett 2012;108:046801.
[33] Park SH, Borme J, Vanegas AL, Corbetta M, Sander D, Kirschner J. ACS Nano 2011;5:8162.
[34] Hämäläinen SK, Sun Z, Boneschanscher MP, Uppstu A, Ijäs M, Harju A, Vanmaekelbergh D, Liljeroth P. Phys Rev Lett 2011;107:236803.
[35] Holstein T. Ann Phys (N Y) 1959;8:325.
[36] Manousakis E. Phys Rev B 1991;44:10991.
[37] Turkevich LA, Holstein TD. Phys Rev B 1987;35:7474.
[38] Hairer E, Nørsett SP, Wanner G. Solving ordinary dierential equations I: nonstiff problems (springer series in computational mathematics). Springer: Berlin; 2010; Press WH, Flannery BP, Teukolsky SA, Wetterling WT. Numerical Recipes: The Art of Scientific Computing. 3rd ed. New York: Cambridge University Press; 2007.